γ-ray spectroscopy of excited states in ^{143}Eu

R. Aryaeinejad, R. B. Firestone,* W. H. Bentley, and Wm. C. McHarris

National Superconducting Cyclotron Laboratory, and Departments of Chemistry and Physics, Michigan State University, East Lansing, Michigan 48824

(Received 11 August 1980)

The level structure of the $N = 80$ nucleus ^{143}Eu has been studied by the ^{144}Sm$(p,2n\gamma)^{143}$Eu reaction using a 30-MeV p beam. We have assigned 37 γ rays deexciting 30 states in ^{143}Eu, placed on the basis of excitation functions and γ-γ coincidence information. Angular distributions were taken at 90°, 100°, 110°, 125°, 140°, and 155° with respect to the beam direction, yielding the A_2 and A_4 coefficients. The in-beam experiments tended to excite higher-spin states than those known from existing β-decay data. Taking the various data together, we could make definite J^π assignments for most of the states in ^{143}Eu. Calculations were performed to explain the resulting level structure in terms of a triaxial weak-coupling model for both prolate and oblate deformations. These calculations indicate that ^{143}Eu has a slight oblate deformation.

[NUCLEAR REACTIONS ^{144}Sm$(p,2n\gamma)^{143}$Eu, E_p= 30 MeV; measured E_γ, I_γ, γ-γ coinc, $\sigma(E_\gamma,\theta)$; deduced ^{143}Eu levels J, π; enriched targets, Ge(Li) detectors; triaxial weak-coupling shell-model calculations.]

I. INTRODUCTION

One of the more interesting regions of the nuclidic chart for current study is the region immediately below the $N=82$ closed shell. Here, long chains of isotones are amenable to study, encompassing both neutron-excess and neutron-deficient nuclei; a wealth of $M4$ and other isomers is available; and a large number of targets is available for cross-comparison in various in-beam experiments. The neutron-deficient $N=80$ isotones are among the most interesting of these nuclei because, although they are close to the major closed shell, they lie at a considerable distance from stability. Thus, they are transitional nuclei; they contain many well-defined shell-model states, but they lie near the edge of the onset of deformation, so many of their higher-lying states can be characterized not only as multiple particle states, but also as (deformed) collective states. Also, the juxtaposition of the $h_{11/2}$ shell-model state with various low-spin states leads to a wealth of both high- and low-spin states in these nuclei.

We have now completed a series of studies on the three odd-mass $N=80$ isotones, $^{143}_{63}$Eu$_{80}$, $^{141}_{61}$Pm$_{80}$, and $^{139}_{59}$Pr$_{80}$, by in-beam γ-ray spectroscopy.[1] These supplement and complement our (and other) previous studies of states in these nuclides excited by β^+/ϵ decay (^{143}Eu, Refs. 2–4; ^{141}Pm, Refs. 5 and 6; and ^{139}Pr, Refs. 7 and 8).

In this paper we report our results on states in ^{143}Eu. By using the in-beam techniques we were able to populate many high-spin states not populated by the β^+/ϵ decay. Many experiments such as γ-γ coincidences, excitation functions for the various γ rays, and angular distributions were carried out in order to construct the final level scheme. In the last sections we attempt to explain the experimental level scheme using a triaxial weak-coupling model described by Meyer-ter-Vehn.[9]

II. EXPERIMENT

A. Target and reaction

The states in ^{143}Eu were excited by the ^{144}Sm$(p, 2n\gamma)^{143}$Eu reaction, using a p beam from the Michigan State University (MSU) (50-MeV) sector-focused cyclotron. The target was prepared by vaporizing Sm enriched to 95.10% ^{144}Sm (obtained from Oak Ridge National Laboratory) onto a thin C backing. The target was 200–300 μg/cm^2 thick and the C backing 25 μg/cm^2 thick.

Excitation functions calculated by the compound-nucleus evaporation code ALICE[10] are shown in Fig. 1. From these it can be seen that the primary contaminants produced directly by the 30-MeV p beam were ^{144}Eu, ^{142}Sm, and, to a lesser extent, ^{142}Eu. Their decays also produced readily identifiable γ rays from states in ^{144}Sm, ^{143}Sm, ^{143}Pm, ^{142}Sm, and ^{142}Nd. These predictions were observed in the experiments and accounted for.

B. γ-ray singles spectra

The ^{143}Eu singles γ-ray spectra were taken with a 10% efficient [with respect to a 7.6×7.6-cm NaI (Tl) detector for the ^{60}Co 1332.513-keV peak; source-to-detector distance, 25 cm] Ge(Li) detector having a resolution of 2.4 keV full width at half maximum (FWHM) (for the ^{60}Co 1332.513-keV peak). They were normally taken at an angle of 125° from the beam direction [to minimize ang-

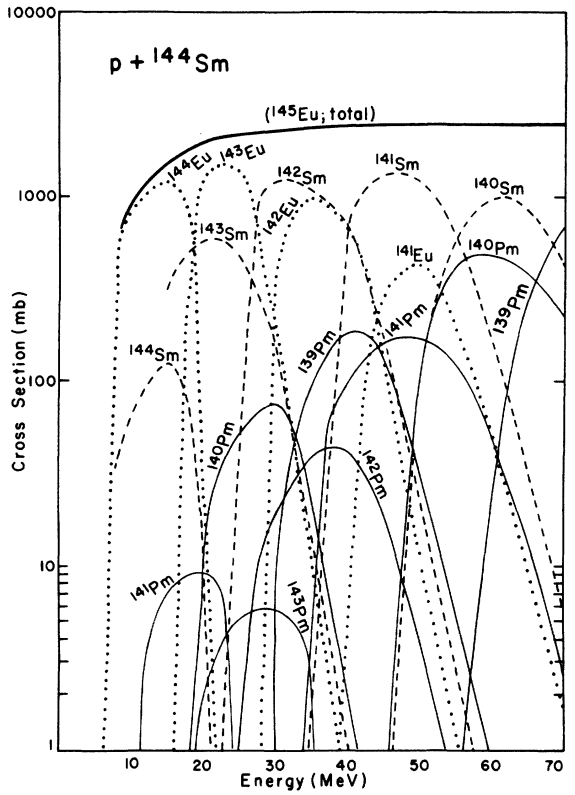

FIG. 1. Excitation functions calculated by the evaporation code ALICE for p's on a ^{144}Sm target. Note that there are two curves for each of the Pm isotopes, one for the evaporation of an α particle, the other for evaporation of $2n + 2p$.

ular distribution effects, 125° being a zero of $P_2(\cos\theta)$]. Typically, a beam current of ≈ 2 nA was used and the detector was placed 20 cm from the target, resulting in a count rate of ≈6000–7000 cps. A singles γ-ray spectrum taken over a 2.5-h period with a 30-MeV p beam is shown in Fig. 2.

A total of thirty-seven γ rays were assigned to ^{143}Eu on the basis of singles spectra and the excitation and coincidence experiments discussed below. These are listed in Table I, together with their relative intensities. Also, Table I includes angular distribution coefficients and conversion coefficients, which will be discussed later. The energy calibrations were performed by counting simultaneously with ^{60}Co, ^{226}Ra, and ^{166}Ho^m radioactive sources and also using some ^{143}Eu γ rays already characterized from ^{143}Gd β^+/ϵ decay as secondary standards. The errors quoted for the energies include estimated errors in the standards and are based primarily on the reproducibility of a peak and its height above background. Where the energies were known more precisely from ^{143}Gd decay, these values were

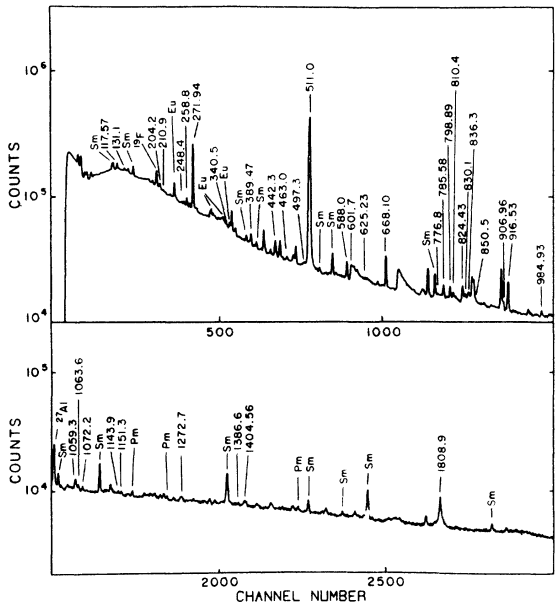

FIG. 2. In-beam singles γ-ray spectrum from the reaction ^{144}Sm$(p, 2n\gamma)^{143}$Eu, using a 30-MeV p beam.

adopted. The errors on the intensities are based primarily on the reproducibility of a given peak.

C. Excitation functions

The γ-ray excitation functions were obtained with p beams having energies of 30, 35, and 40 MeV. The γ rays were detected with the 10% efficient Ge(Li) at ≈90° from the beam direction and 5 cm from the target. The beam intensity was held as constant as possible (±20%) from experiment to experiment, the integrated beam-current was recorded, and a pulser was included in the spectra to allow reliable normalization of the spectra from one experiment to another. The results for seven prominent γ rays are shown in Fig. 3, where the intensities have been normalized to the intensity from the 30-MeV reaction. (It should be mentioned that this excitation function procedure was also very useful in eliminating impurity γ rays from competing reactions.)

D. Coincidence spectra

The γ-γ coincidence spectra were obtained with a 30-MeV p beam. The 10%-efficient Ge(Li) detector and a 7.7%-efficient Ge(Li) detector (energy resolution 1.9 keV FWHM) were used. A standard three-parameter ($E_\gamma \times E_\gamma \times t$) fast-slow coincidence setup with constant-fraction timing was used. The coincidences were recorded event-by-event on magnetic tape for off-line sorting with background subtraction. (For more details, see Ref. 1).

TABLE I. Energies, relative intensities, angular-distribution coefficients, and multipolarities for γ transitions in ^{143}Eu from in-beam studies.

E_γ (keV)	I_γ	Angular distribution coefficients A_2/A_0	A_4/A_0	Multipolarity (from conversion electrons, Ref. 3)
117.57 ± 0.05 [a]	3.7 ± 0.2	isotropic		$M2$
131.1 ± 0.1 [a]	0.30 ± 0.08	0.10 ± 0.03		
204.77 ± 0.05 [a]	5.0 ± 0.4	isotropic		
210.9 ± 0.1 [a]	1.1 ± 0.3	−0.55 ± 0.12		$M1$
248.4 ± 0.1	1.6 ± 0.2	−0.39 ± 0.10	0.15 ± 0.10	
258.1 ± 0.03 [a]	7.7 ± 0.5			$M1$ (or $E3$)
271.94 ± 0.03 [a]	≡100	isotropic		$M1$
340.5 ± 0.3	1.0 ± 0.1			
389.47 ± 0.05 [a]	1.5 ± 0.2	isotropic		$E3$
442.3 ± 0.1	11.9 ± 0.8			
463.7 ± 0.1	2.8 ± 0.2			
497.3 ± 0.1 [a]	weak			
588.00 ± 0.03 [a]	12.7 ± 0.8	−0.41 ± 0.02	0.03 ± 0.02	$M1+E2$
601.7 ± 0.2	7.5 ± 0.7	0.9 ± 0.4		
625.23 ± 0.08 [a]	weak			
668.10 ± 0.03 [a]	27.3 ± 1.6	−0.68 ± 0.03	−0.02 ± 0.04	$M1+E2$
776.8 ± 0.1 [a]	weak			$M1$ (or $E3$)
785.56 ± 0.06 [a]	8.7 ± 0.5	0.23 ± 0.06	−0.04 ± 0.03	$E2$
798.89 ± 0.06 [a]	8.2 ± 0.5	−0.22 ± 0.01	−0.09 ± 0.02	$E2$
810.4 ± 0.2	1.6 ± 0.3			
824.43 ± 0.09 [a]	10.3 ± 0.6	0.09 ± 0.02	−0.02 ± 0.06	$E2$
830.1 ± 0.1 [a]	weak			
836.3 ± 0.1 [a]	4.2 ± 0.3			
850.5 ± 0.1	1.8 ± 0.3			
906.96 ± 0.06 [a]	5.6 ± 0.6			$E2$
916.53 ± 0.05 [a]	2.4 ± 0.4	0.31 ± 0.03	−0.03 ± 0.04	$E2$
984.93 ± 0.05 [a]	3.9 ± 0.3	0.15 ± 0.08	0.06 ± 0.10	$M1+E2$
1059.3 ± 0.1 [a,b]	8.3 ± 0.5	0.24 ± 0.04	−0.07 ± 0.05	
1063.6 ± 0.1	3.2 ± 0.3	0.39 ± 0.10		
1072.2 ± 0.1	2.4 ± 0.3	0.27 ± 0.14		
1143.9 ± 0.1	2.0 ± 0.2			
1151.3 ± 0.1	2.4 ± 0.3			
1272.7 ± 0.2	2.3 ± 0.3	−0.15 ± 0.10	0.08 ± 0.06	
1386.7 ± 0.6	0.20 ± 0.05			
1404.56 ± 0.07 [a]	3.6 ± 0.3			
1807.14 ± 0.07 [a]	19.6 ± 1.3	0.72 ± 0.48		

[a] These γ rays were also seen in the decay of ^{143}Gd, where the precision in energy was greater. The in-beam studies yielded essentially the same energies, so we have adopted the more precise energy values from Ref. 2.

[b] There are two 1059.3-keV transitions in the level scheme; see text.

Some coincidence spectra are shown in Fig. 4. The integral coincidence spectrum [all coincidence events as displayed from the 10% Ge(Li) detector] is at the top, and three representative gated spectra are shown below it. Because of the relatively larger backgrounds that had to be subtracted from these gated spectra, they were smoothed (three-channel) to enhance the peaks. (The raw spectra and the complete set of gated spectra are shown in Ref. 1.) A summary of the coincidence data is given in Table II.

E. γ-ray angular distributions

The p-beam energy for obtaining the γ-ray angular distributions was again 30 MeV. The 10%-efficient Ge(Li) detector was rigidly mounted with its cryostat on the arm of a goniometer with the face of the detector 15 cm from the target. The data were collected at 90°, 100°, 110°, 125°, 140°, and 155° with respect to the beam direction. The angles were taken in random order for the various experiments, and data were

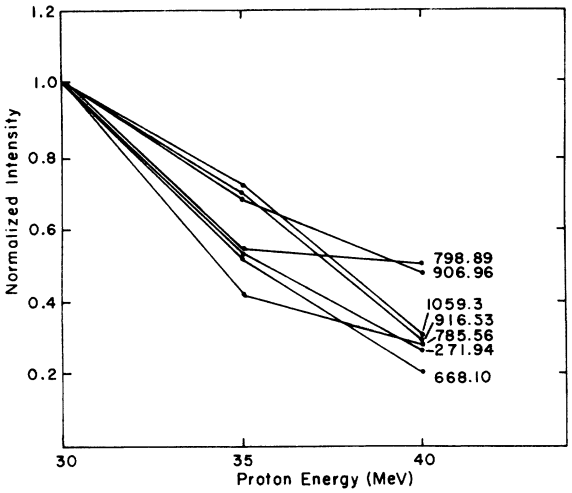

FIG. 3. Excitation functions for seven of the more prominent ^{143}Eu γ rays.

typically collected for 2.5 h at each angle.

The 271.94- and 117.57-keV isotropic transitions were used as an internal normalization for the spectra taken at different angles. After the normalization of the γ-ray peak areas, least-squares fits to the experimental angular distributions were made using the computer code GADFIT.[11] The fits were made to the equation:

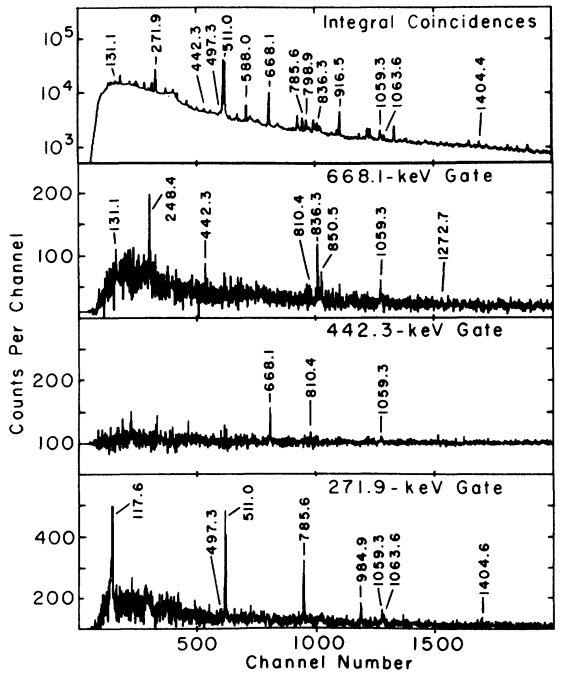

FIG. 4. In-beam γ-γ coincidence spectra for the reaction ^{144}Sm$(p, 2n\gamma)^{143}$Eu. The integral coincidence spectrum "all events" is shown at the top, and three representative smoothed gated spectra are shown underneath.

TABLE II. Summary of coincidence results for the ^{144}Sm$(p, 2n\gamma)^{143}$Eu reaction.

Gated γ rays (keV)	Coincident γ rays (keV)
117.57	271.94
131.1	668.10
204.2	258.8, 340.2
210.9	588.00
248.4	668.10
258.8	204.2, 340.2
271.94	117.57, 497.3, 785.56, 984.93, 1059.3, 1063.6, 1404.56
340.2	204.2, 258.8, 463.0
389.47	
442.3	668.10, 810.4, 1059.3
463.0	340.2
497.3	271.94, 984.93
588.00	210.9, 625.23, 776.8
601.7	916.53
625.23	588.00
668.10	131.1, 248.4, 442.3, 810.4, 836.3, 850.5, 1059.3, 1272.7
776.8	588.00
785.56	271.94, 1063.6
798.89	830.1
810.4	442.3, 668.10
824.43	1143.9, 1386.69
830.1	798.89
836.3	668.10
850.5	668.10
906.96	
916.53	601.7, 1072.2
984.93	271.94, 497.3
1059.3[a]	271.94, 442.3, 668.10
1063.6[b]	271.94, 668.10, 785.56
1072.2	916.53
1143.9	824.43
1151.3	916.53
1272.7	668.10
1386.69	824.43
1404.56	271.94
1808.9	

[a] There are two separate ≈1059.3-keV γ's.
[b] Perhaps there are also two separate ≈1063.6-keV γ's.

$$I = 1 + (A_2/A_0)P_2(\cos\theta) + (A_4/A_0)P_4(\cos\theta).$$

The parameters extracted from the fit, A_2/A_0 and A_4/A_0, are included in Table I. Angular distribution coefficients not listed in the tables were for transitions that were very weak or that were parts of multiplets and consequently had very large errors. Where a good fit for A_4/A_0 could not be obtained, the data were refit with the value for A_4/A_0 set equal to 0. Some representative angular distributions, together with their calculated fits, are shown in Fig. 5.

III. THE ^{143}Eu LEVEL SCHEME

Coincidence information, intensity balances, conversion coefficients, and excitation functions

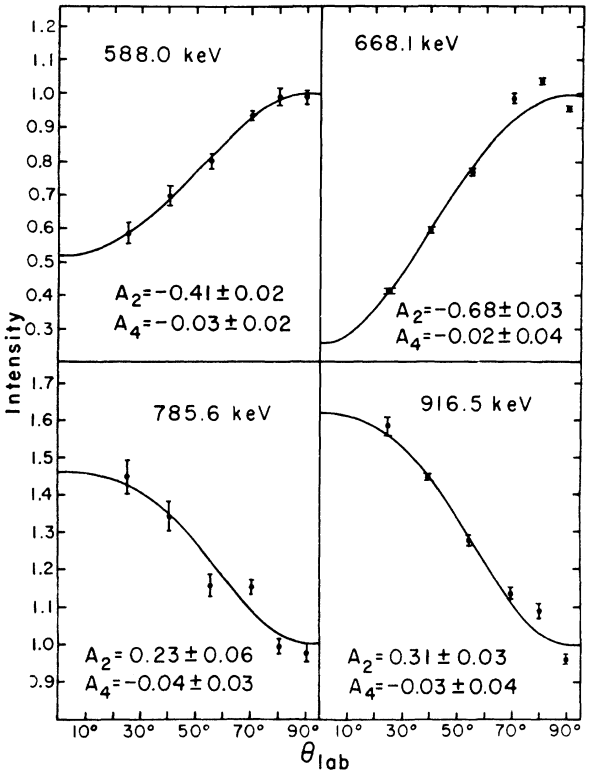

FIG. 5. Four representative angular distributions of ^{143}Eu γ rays, together with their fits calculated by the code GADFIT. The points correspond to 90° and the backward angles, 100°, 110°, 125°, 140°, and 155°.

for individual γ rays were the primary factors used to construct a level scheme for ^{143}Eu. Secondary factors were energy summing relationships, input from the known ^{143}Gd^{m+g} decay scheme,[2] and our angular distribution data. The spin and parity assignments were made on the basis of angular distribution coefficients, conversion coefficients, and input from the ^{143}Gd^{m+g} decay scheme. The resulting level scheme is shown in Fig. 6. For comparison, the level schemes of ^{143}Eu obtained from the decay of ^{143}Gd^{m+g} are shown in Fig. 7. Specific details of the construction of the level scheme and J^π assignments are discussed next.

Ground, 271.94-, and 389.47-keV states. The most intense γ transition in the in-beam, as well as the off-line, experiments is the 271.94-keV transition, which is in coincidence with the 117.57-keV transition (and with six others—see Table II). On the other hand, no other γ rays appear to be in coincidence with the 117.57-keV transition. This leads to the adoption of a cascade, with the 117.57-keV transition on top of the 271.94-keV transition, and places states at 271.94 and 389.51 keV. The upper state is also depopulated directly by the 389.47-keV transition, and we adopt this energy for the state.

The ground state has been reported[12] to have $J^\pi = \frac{5}{2}^+$, and 271.94- and 389.47-keV states have been assigned $\frac{7}{2}^+$ and $\frac{11}{2}^-$, respectively, on the basis of the multipolarities of the three above γ transitions and the logft values for ^{143}Gd^m β decay. Also, in the ^{143}Gd^m decay studies, the 389.47-keV state was measured to have a half-life of 50.0±0.5 μsec. In our present work we found the 117.57- and 271.94-keV transitions to be definitely isotropic and the weaker 389.47-keV transition probably isotropic. Although this information does not allow us to comment further on the J^π assignments, it is consistent with the long half-life of the 389.47-keV state (plus the complex feeding into the 271.94-keV state).

The ground, 271.94-, and 389.47-keV states thus should consist primarily of the $\pi d_{5/2}$, $\pi g_{7/2}^{-1}$, and $\pi h_{11/2}$ single-particle states.

258.81-, 463.7-, and 804.1-keV states. The other set of low-lying states, presumably of lower spin, has the interconnecting transitions of 204.77, 258.81, 340.5, and 463.7 keV. Coincidence relations among them and the intensity balances lead to the placement of levels at 258.81, 463.7, and 804.1 keV. The first two were observed in ^{143}Gd^g decay; the 804.1-keV state has not been previously observed.

Spin assignments for these states were not possible from angular distribution coefficients because all the γ transitions were very weak and had large errors on the values for the transition intensities. However, the 258.81- and 463.7-keV states were assigned $\frac{3}{2}^+$ and $\frac{1}{2}^+$, respectively, from ^{143}Gd^g decay. Presumably the major component of the 463.7-keV state is the $\pi s_{1/2}$ single-particle state; however, the 258.81-keV state is of a more complicated nature—it is discussed more thoroughly in Sec. IV.

We cannot say much about the 804.1-keV state. Its connection to the 463.7-keV state tells us more that it is related to the $s_{1/2}$ state than what its spin is. For example, it might be $[2^+ \otimes s_{1/2}]_{1/2^+,3/2^+,5/2^+}$—any one of these would selectively deexcite to the 463.7-keV state. On the other hand, one might anticipate some feeding from the many higher-lying $\frac{9}{2}$ states (see below) to a $\frac{5}{2}$ state, making $\frac{1}{2}^+$ or $\frac{3}{2}^+$ the preferred assignment. Arguments based on missing transitions are rather weak, however, so we are more safely left with the possibilities $\frac{1}{2}$, $\frac{3}{2}$, or $\frac{5}{2}$.

977.47-keV state. This state feeds into the $\frac{11}{2}^-$ 389.47-keV state by the 588.00-keV transition. (Although the 50.0-μsec $t_{1/2}$ of the 389.47-keV state makes this impossible to confirm by a direct coincidence measurement, the other coin-

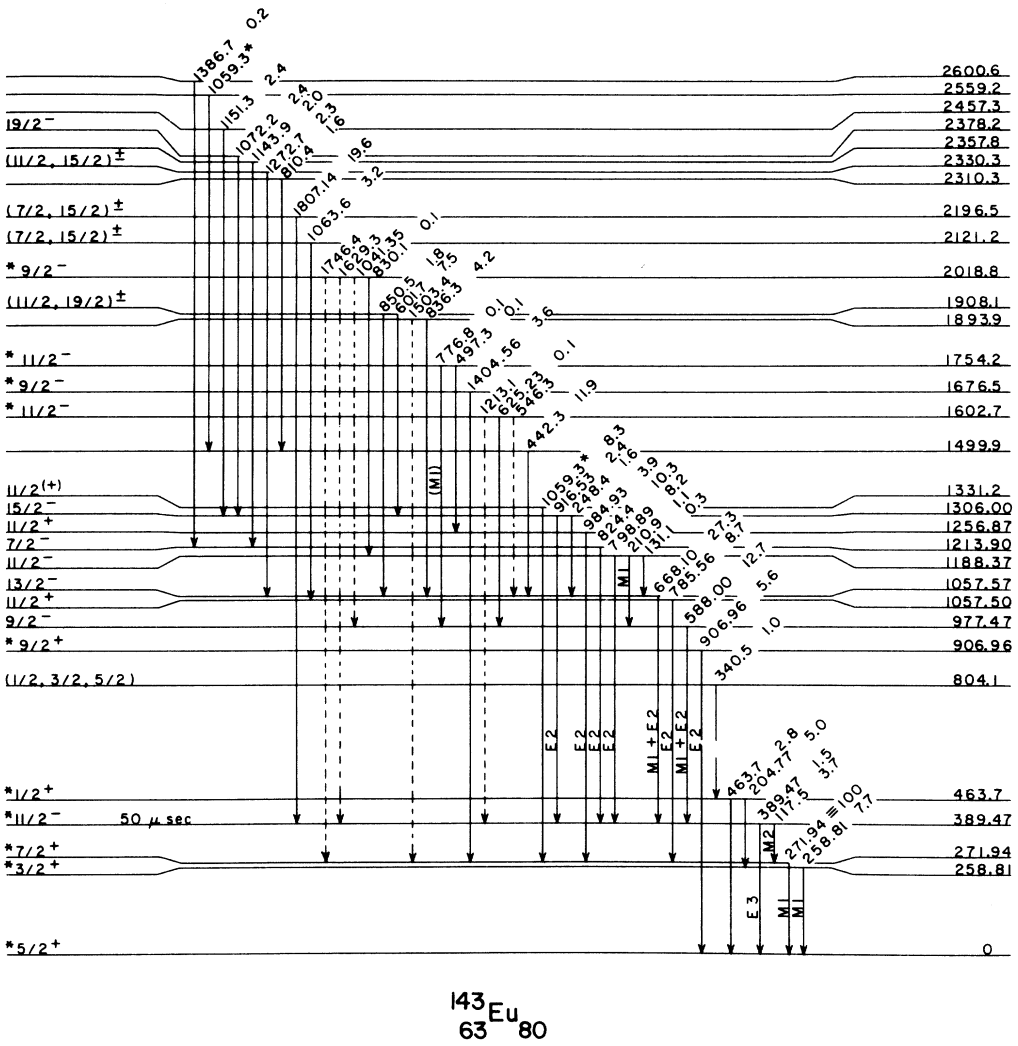

FIG. 6. ^{143}Eu level scheme as determined by the ^{144}Sm$(p, 2n\gamma)^{143}$Eu reaction. The asterisks before J^π assignments indicate that we relied heavily on the ^{143}Gd^{m+g} β^+/ϵ decay (Ref. 2) for these assignments. Also, the dashed γ transitions are weak transitions seen in ^{143}Gd^{m+g} decay but not seen in our in-beam studies; however, they originate from levels seen in the in-beam studies. It should be noted that there are two 1059.3-keV transitions in this level scheme.

cidence relations with the 588.00-keV γ confirm this placement, as did the extensive coincidence relations from ^{143}Gd^m decay.) From ^{143}Gd^m decay the 977.47-keV state was tentatively assigned $\frac{7}{2}^-$. However, if the 588.00-keV transition is a mixed $M1/E2$ transition (Table I), the J^π assignment is restricted to $\frac{9}{2}^-$, $\frac{11}{2}^-$, or $\frac{13}{2}^-$. The $\frac{11}{2}^-$ value is ruled out because of the large negative value of A_2 and the small positive value of A_4. The fact that this state is not fed by γ rays from high-spin states indicates that it most likely is not in the yrast sequence, eliminating $J^\pi = \frac{13}{2}^-$. (Below we shall show that the 1057.57-keV state has $J^\pi = \frac{13}{2}^-$ and receives feeding from the high-spin states. It thus appears to be the $\frac{13}{2}^-$ yrast state, making the possibility of a lower-lying $\frac{13}{2}^-$ state unlikely.) We thus assign this state $\frac{9}{2}^-$.

1057.50-keV state. The coincidence information between the 785.56- and 271.94-keV γ's places this state. It was also seen in ^{143}Gd^m decay, where it was tentatively assigned $\frac{9}{2}^+$ or $\frac{11}{2}^+$. The $E2$ multipolarity of the 785.56-keV transition allows J^π values from $\frac{3}{2}^+$ to $\frac{11}{2}^+$. The angular distribution data for this transition, however, can be fit by only two values, $\frac{3}{2}^+$ or $\frac{11}{2}^+$. (The positive value of A_2 and small but negative value of A_4 tell us the transition is a stretched $E2$, eliminating an otherwise possible $\frac{7}{2}^+$.) From ^{143}Gd^m decay $\frac{3}{2}^+$ can clearly be ruled out, leaving $J^\pi = \frac{11}{2}^+$ for this state.

1057.57-keV state. Again, the 50-μsec $t_{1/2}$ of the 389.47-keV state prevents a direct coincidence

measurement to place the 1057.57-keV level feeding into it, but the eight other transitions seen in coincidence with the 688.10-keV transition place the 1057.57-keV level quite securely. (This type of argument will not be belabored henceforth but applies equally well to many of the states discussed below.) This level was also placed in ^{143}Gd^{m} decay and tentatively assigned $\frac{13}{2}^{+}$. The $M1+E2$ mixed multipolarity of the 688.10-keV transition limits its J^{π} to $\frac{9}{2}^{-}$, $\frac{11}{2}^{-}$, or $\frac{13}{2}^{-}$. The large negative A_2 and small A_4 rule out $\frac{11}{2}^{-}$. Since the 668.10-keV γ is seen so intensely in our in-beam experiments, yrast arguments lead us to prefer the higher spin, i.e., $\frac{13}{2}^{-}$, for this state.

1188.36-keV state. This state, placed by coincidence information from its deexciting 131.1- and 210.9-keV transitions, was confirmed by the strong 798.89-keV transition feeding the $\frac{11}{2}^{-}$ 389.47-keV state. The pure $E2$ multipolarity of the latter transition could indicate a stretched quadrupole transition, but the negative A_2 and A_4 values establish it to be a $J \rightarrow J$ pure quadrupole transition. Its J^{π} would thus be $\frac{11}{2}^{-}$. We believe the tentative $\frac{9}{2}^{-}$ assignment reached from ^{143}Gd^{m} decay data to be incorrect because the negative A_4 value also rules out a mixed $E1/E2$ multipolarity for the 798.89-keV transition.

1213.90-keV state. The 824.43-keV transition that deexcites this state to the $\frac{11}{2}^{-}$ 389.47-keV state is an $E2$, which limits its J^{π} to $\frac{7}{2}^{-}$ through $\frac{15}{2}^{-}$. The angular distribution coefficients limit this further to $\frac{7}{2}^{-}$. (The value of A_2 is too small for a $\frac{15}{2}^{-} \rightarrow \frac{11}{2}^{-}$ transition; cf. the 785.56-keV transition from the 1057.50-keV state.) This state was left unassigned in the ^{143}Gd^{m} decay studies; $J^{\pi}=\frac{7}{2}^{-}$ should not be allowed with a logft value of 6.5. However, if we assume that much of the intensity of the 824.43-keV transition in ^{143}Gd^{m} decay results from missing undetected transitions from higher-lying states,[13] then we expect a considerably higher logft value, consistent with the $\frac{7}{2}^{-}$ assignment.

1256.87-keV state. For the 984.93-keV transition that deexcites this state to the $\frac{7}{2}^{+}$ 271.94-keV state, Wisshak *et al.*[3] assigned $M2+E3$ mixed multipolarity. According to the argument in Ref. 2, this assignment was wrong because of the use of an incorrect α_K value—the latter calculation indicated $M1+E2$ multipolarity. Our in-beam angular distribution results are consistent with a (stretched) quadrupole transition. Since the experimental α_K is $(6.9\pm1.4)\times10^{-3}$, and the calculated[14] α_K is 1.6×10^{-2} for an $M2$ and 3.4×10^{-3} for an $E2$ transition, the $M2$ can be excluded. Thus, the 1256.87-keV state has $J^{\pi}=\frac{11}{2}^{+}$.

1306.00-keV state. The 916.53-keV transition

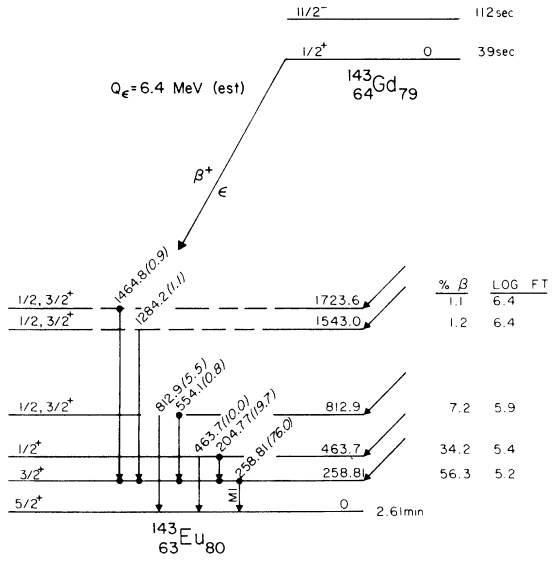

FIG. 7. Decay schemes of ^{143}Gd^{g} and ^{143}Gd^{m} from Ref. 2 for comparison with our in-beam studies.

(although it has a fairly large error in intensity) deexciting this state appears to be a pure stretched $E2$. Its angular distribution pattern restricts the J^{π} value of the state to $\frac{7}{2}^{-}$ or $\frac{15}{2}^{-}$. Yrast considerations lead us to prefer the larger value of $\frac{15}{2}^{-}$. (Also, the A_2 is uncomfortably large for a $J \rightarrow J+2$ transition.)

1331.2-keV state. The J^{π} of this state is restricted to $\frac{3}{2}^{\pm}$ or $\frac{11}{2}^{\pm}$ because of the angular distribution coefficients of the 1059.3-keV transition (whose multipolarity has not been determined). The $\frac{3}{2}^{\pm}$ value can be ruled out because the $(p, 2n\gamma)$ reaction is not likely to populate low-spin states at higher excitation energies. (Also, again the A_2 appears to be too large for a $J \rightarrow J+2$ transition.) From the ^{143}Gd^{m} decay data we can also exclude $\frac{3}{2}^{\pm}$. An $\frac{11}{2}^{-}$ assignment would require the 1059.3-keV transition to be $M2$ and, although this cannot be definitely ruled out, we prefer the $\frac{11}{2}^{+}$ assignment. (Also, see the remarks below about a second, weaker 1059.3-keV transition.)

2378.2-keV state. This state, the last one for which we were able to make a unique J^{π} assignment from our in-beam data, has its J^{π} restricted to $\frac{11}{2}^{-}$ or $\frac{19}{2}^{-}$ because of the large A_2 value. Its decay solely to the $\frac{15}{2}^{-}$ state and its large population in the $(p, 2n\gamma)$ reaction lead us to prefer $\frac{19}{2}^{-}$.

Other states. The remaining states in the level scheme in Fig. 6 were placed on the basis of coincidence data, corroborated by β-decay data and energy sums. Their J^{π} values could not be determined uniquely from our present exper-

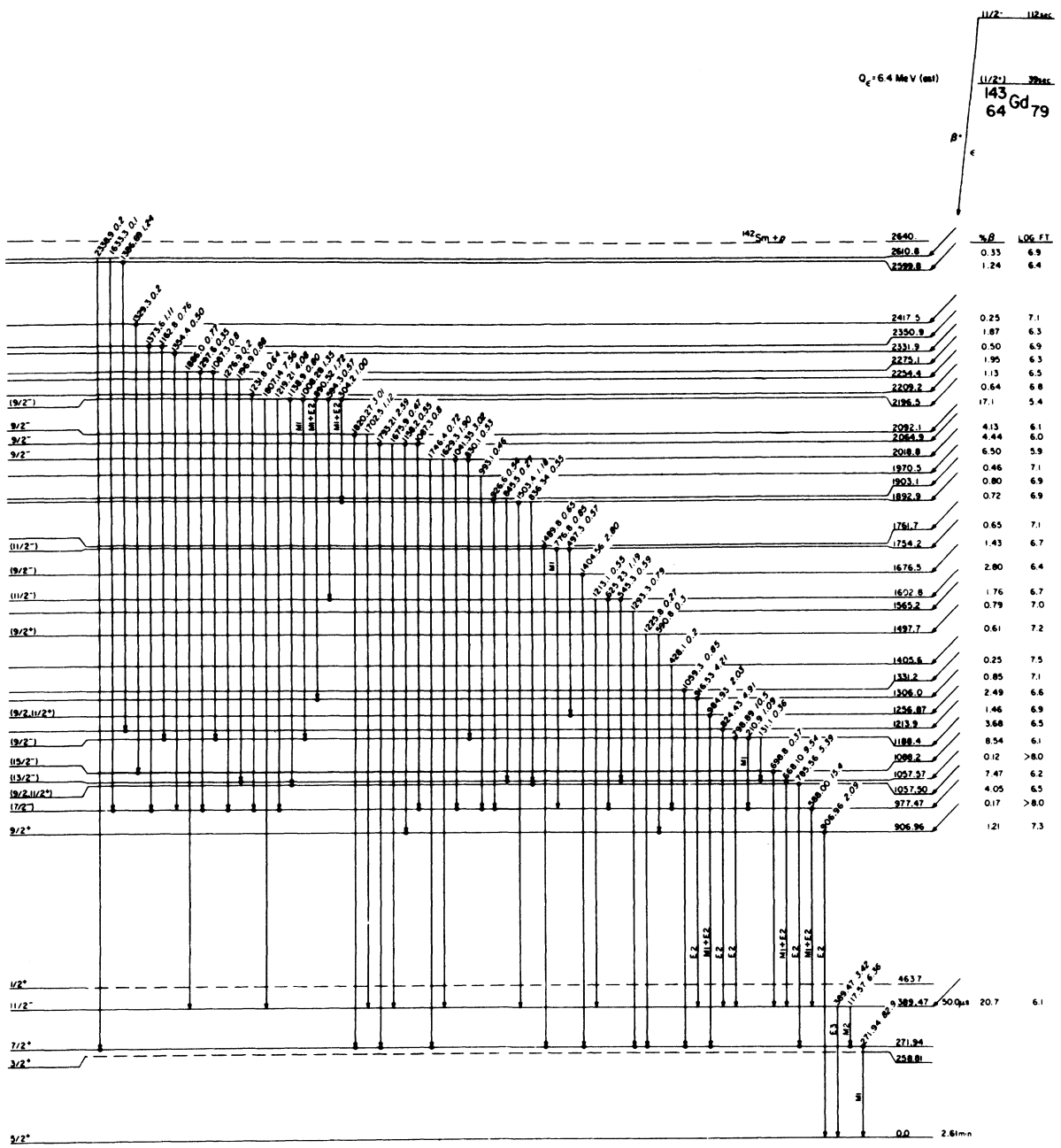

FIG. 7. (*Continued*)

imental data. However, some J^π values could be excluded on the basis of our angular distributions. Also, some of these states observed in our in-beam work had their assignments made from $^{143}Gd^m$ decay—these are indicated by asterisks on the level scheme. And six transitions have been included (dashed lines) that were seen in $^{143}Gd^m$ decay but not in the in-beam experiments. It is worth mentioning that there are two 1059.3-keV transitions: in addition to the one deexciting the 1331.2-keV state (see above), coincidence data indicate another, weaker one deexciting a state at 2559.4 keV.

IV. DISCUSSION

A total of 31 states in $^{143}_{63}Eu_{80}$, many of which had not been populated by ^{143}Gd β decay,[2,3] were

deduced from our in-beam γ-ray experiments. For the purposes of discussion these states can be classified in three categories: (1) single-quasiparticle states, (2) negative-parity collective states, and (3) positive-parity collective states.

A. Single-particle states

The four states at 0, 271.94, 389.47, and 463.7 keV can, as expected, be described as consisting primarily of the $\pi d_{5/2}$, $\pi g_{7/2}^{-1}$, $\pi h_{11/2}$, and $\pi s_{1/2}$ single-quasiparticle states, respectively—four of the five possible single-proton states between $Z=50$ and $Z=82$. These states have not been confirmed as single-particle states by direct transfer reactions (no target exists for a straightforward reaction), but similar states have been populated with large spectroscopic factors at comparable positions in $N=82$ nuclei.[15] These four states in the $N=82$ isotones have also been successfully analyzed by de Takacsy and Das Gupta[16] as single-quasiparticle states.

It is important here to mention that the $\frac{3}{2}^+$ state at 258.81 keV probably does not consist primarily of the $\pi d_{3/2}$ single-quasiparticle state. The major component of the $\pi d_{3/2}$ state, which is more fractionated than the other four single-proton states, lies above 400 keV in the other $N=80$ odd-mass isotones.[17] Thus, it is unlikely that it should lie at such a low energy in ^{143}Eu. (A state observed at 812.9 keV from ^{143}Gd$^{\varepsilon}$ decay may very well contain a major portion of the $\pi d_{3/2}$ wave function.) Also, our calculations (discussed below) show the 258.81-keV state to consist primarily of the $\pi d_{5/2}$ state coupled to the 2^+ ^{142}Sm core.

B. Negative-parity collective states

There are a number of equivalent ways, it is hoped, to describe and interpret the more complex, higher-lying states for odd-mass nuclei in this general region. From the standpoint of β decay alone, a three-quasiparticle (or multi-quasiparticle) approach has worked quite well,[5,7,18] and it has the advantage of simplicity, almost an exaggerated simplicity. The other extreme of this picture is to use a weak coupling (decoupling) model in which the single-quasiparticle states are coupled to simple phonon excitations of the ^{142}Sm core. A rather qualitative version of this, using the five single-proton states coupled to the 2_1^+, 0_2^+, 2_2^+, 4_1^+, and 3_1^- vibrational states, was discussed in Ref. 2. The two most noteworthy recent quantitative approaches are the triaxial weak-coupling model described by Meyer-ter-Vehn[9] and the interacting boson-fermion model of collective states developed and described by Iachello and Scholten.[19] We have performed calculations using a computer code modified from that of Meyer-ter-Vehn. Unfortunately, the only calculations of Iachello and Scholten completed at this data relate to the odd-mass Eu isotopes *above* $N=82$. Thus, we limit our discussion here to the triaxial weak-coupling model and hope that in the near future the interacting boson-fermion calculations can be extended to ^{143}Eu and its neighbors.

The negative-parity collective states in ^{143}Eu are expected to consist primarily of the $\pi h_{11/2}$ state coupled to a triaxial core. The lowest excited states of the adjacent even-even nucleus (Ref. 17), ^{142}Sm, were used in order to determine the deformation parameter β and the asymmetry parameter γ. Since the triaxial model applied to the even-even neighbor(s) does not distinguish between prolate ($0° \leq \gamma < 30°$) and oblate ($30° < \gamma \leq 60°$) deformations, we performed calculations for both types. Our results are shown in Fig. 8.

For a prolate shape ($\gamma = 23.5°$), the agreement with experiments is not good, either in the energy separations or even in the ordering of the levels. The calculated energies of the second $\frac{11}{2}^-$ state (1897.0 keV), the first $\frac{9}{2}^-$ state (1186.0 keV),

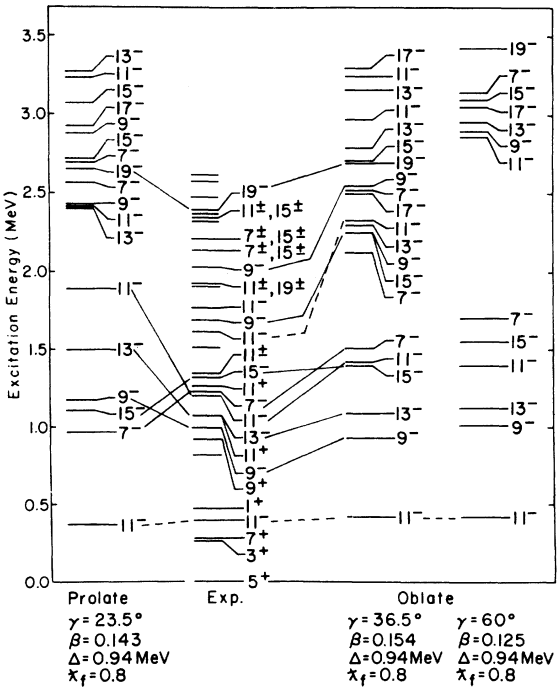

FIG. 8. Energies of calculated excited negative-parity states in ^{143}Eu compared with our experimental findings. We calculated these energies using a triaxial weak-coupling model (Ref. 9) coupling the $\pi h_{11/2}$ state to a deformed core. Results for both prolate and two different oblate deformations are shown; a slight oblate deformation seems indicated.

and the first $\frac{13}{2}^-$ state (1508.0 keV) are considerably greater than the experimental values. Also, the prolate calculation places the first $\frac{7}{2}^-$ state at 979.0 keV; if it were lying this low, it should have been seen experimentally. These contradictions place doubt on ^{142}Eu being prolate. Actually, a prolate-oblate shape transition between $N=77$ and $N=79$ in the $_{60}$Nd isotopes has been reported by Gizon *et al.*,[20] so we might anticipate ^{143}Eu to be oblate.

Calculations were made for oblate shapes at both $\gamma=36.5°$ (60°−23.5°) and $\gamma=60°$. The agreement with experiments is much improved, both in the level ordering itself and in the energy separations of the lower states, with the exception of the first $\frac{15}{2}^-$ state. The calculated energies of the first $\frac{9}{2}^-$ (900.0 keV), first $\frac{13}{2}^-$ (1058.0), first $\frac{15}{2}^-$ (1365.0), second $\frac{11}{2}^-$ (1386.0), first $\frac{7}{2}^-$ (1472.0), and first $\frac{19}{2}^-$ (2655.0) states at $\gamma=36.5°$ confirm the oblate shape for ^{143}Eu. Additional evidence for triaxiality includes the second and third $\frac{11}{2}^-$ (1386.0- and 2295.0-keV) states, as well as the second and third $\frac{9}{2}^-$ (2220.0- and 2506.0-keV) states, in decent agreement with their experimental counterparts. Thus, the higher-lying states appear to favor a triaxial description in preference to a pure oblate shape.

C. Positive-parity collective states

The positive-parity states can also be generated by coupling the $\pi d_{5/2}$, $\pi g_{7/2}^{-1}$ states to the triaxial core. Here the results are considerably poorer because of the ease of mixing with close-lying states having the same positive parity. In Fig. 9 we show the results of our calculations for coupling "pure" $\pi d_{5/2}$ and $\pi g_{7/2}^{-1}$ to the ^{142}Sm core, using the oblate shape γ of 36.5°.

The $\pi d_{3/2}$ coupling leads to the $\frac{3}{2}^+$ state at 258.81 keV. This indicates that the 258.81-keV state is primarily a collective state and not the $\pi d_{3/2}$ single-quasiparticle state. In fact, the $\pi d_{3/2}$ state has been observed[24] at 405.0 and 403.9 keV, respectively, in $^{139}_{59}$Pr and $^{141}_{61}$Pm, and lies even higher in the other $N=80$ odd-mass isotones.

The calculated $\frac{1}{2}^+$ state from the $\pi d_{5/2}$ coupling lies at 789.0 keV and could correspond to either the 804.1-keV state observed in our experiments or the 812.9-keV state observed in ^{143}Gd$^{\varepsilon}$ decay. The first $\frac{3}{2}^+$ and second $\frac{1}{2}^+$ state from this coupling are predicted to lie at 1546.0 and 1929.0 keV, respectively. We excited no such low-spin states near these energies in our in-beam experiments, but the two $\frac{1}{2}^+$ or $\frac{3}{2}^+$ states found at 1543.0 and 1723.6 keV from ^{143}Gd$^{\varepsilon}$ decay might have a loose correspondence to them.

The $\pi g_{7/2}^{-1}$ coupling predicts the first $\frac{11}{2}^+$ state to lie at 1061.0 keV. This corresponds to the experimental state found at 1057.50 keV.

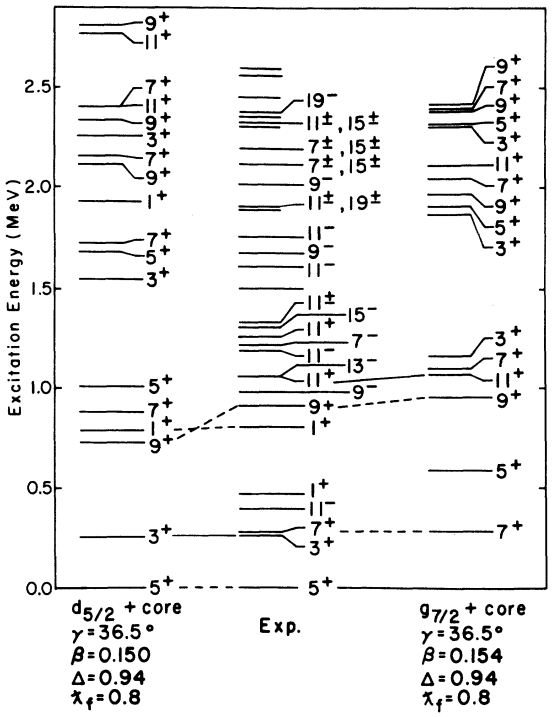

FIG. 9. Energies of calculated excited positive-parity states in ^{143}Eu compared with our experimental findings. We calculated these energies using a triaxial weak-coupling model (Ref. 9), coupling both the $\pi d_{5/2}$ and $\pi g_{7/2}^{-1}$ states to an oblately deformed core.

Finally, the $\pi d_{5/2}$ coupling predicts a $\frac{9}{2}^+$ state lying at 732.9 keV, and the $\pi g_{7/2}^{-1}$ coupling predicts one at 950 keV. The experimentally observed $\frac{9}{2}^+$ state at 906.96 keV deexcites directly to the ground state and not through the 271.94-keV state. This leads us to believe that it consists primarily of the $\pi d_{5/2}$ coupling.

Little can be said about the higher-lying positive-parity states; first, because of the lack of information that can tie down specific spin assignments, and, second, because of the strong mixing of these positive-parity states with one another.

D. Conclusion

The triaxial weak-coupling model seems to do an unexpectedly good job of describing the level structure in ^{143}Eu. The calculations for negative-parity states indicate an oblate shape, and those for positive-parity states gave at least a germinal fit. In order to test it further, we are now extending our systematics to the study of $^{141}_{61}$Pm$_{80}$ and $^{139}_{59}$Pr$_{80}$, each nucleus by both the $(p, 2n\gamma)$ reaction and the complementary $(\alpha, 4n\gamma)$ reaction. Our results and systematics should be forthcoming shortly.

ACKNOWLEDGMENTS

We wish to thank members of the nuclear spectroscopy groups at the MSU National Superconducting Cyclotron Laboratory for their aid in obtaining, analyzing, and interpreting our data. In particular, we thank Dr. Phil Walker for most helpful discussions and for a critical reading of the manuscript. This material is based upon work supported by the U.S. National Science Foundation under Grants No. PHY 76-04912 and PHY 78-01684.

---

*Present address: Nuclear Science Division, Lawrence Berkeley Laboratory, Berkeley, Calif. 94720.

[1]R. Aryaeinejad, Ph.D. thesis, MSU, 1980, MSU Report No. MSUNC-210, 1980 (unpublished).

[2]R. B. Firestone, R. A. Warner, Wm. C. McHarris, and W. H. Kelly, Phys. Rev. C 17, 718 (1978).

[3]K. Wisshak, A. Hanser, H. Klewe-Nebenius, J. Buschmann, H. Rebel, H. Faust, H. Toki, and A. Fässler, Z. Phys. A 277, 129 (1976).

[4]J. Van Klinken, D. Hales, H. Klewe-Nebenius, K. Wisshak, G. Nawicki, J. Buschmann, S. Göring, R. Löhken, H. Rebel, and G. Schatz, Gesellschaft für Kernforschung Karlsruhe, Report No. KFK 1768, 1973 (unpublished).

[5]R. E. Eppley, R. R. Todd, Wm. C. McHarris, and W. H. Kelly, Phys. Rev. C 5, 1084 (1972).

[6]G. G. Kennedy, J. Deslauriers, S. C. Gujrathi, and S. K. Mark, Phys. Rev. C 15, 792 (1977).

[7]D. B. Beery, W. H. Kelly, and Wm. C. McHarris, Phys. Rev. 188, 1851 (1969).

[8]V. S. Butsev, Ts. Vylov, V. G. Kalinnikov, N. A. Tikhonov, and E. Herrmann, Izv. Akad. Nauk Arm. SSSR, Ser. Fiz.-Mat. Nauk 35, 1618 (1971).

[9]J. Meyer-ter-Vehn, Nucl. Phys. A249, 111 (1975).

[10]M. Blann and F. Plasil, nuclear evaporation code ALICE, adapted for the MSU NSCL Sigma-7 computer by W. Bentley.

[11]GADFIT, computer code written by R. A. Warner, for the MSU NSCL Sigma-7 computer.

[12]C. Ekström, S. Ingelman, M. Olsmats, and B. Wannberg, Phys. Scr. 6, 181 (1972).

[13]This problem is discussed in R. B. Firestone, R. C. Pardo, and Wm. C. McHarris, Phys. Lett. 89B, 36 (1979).

[14]R. S. Hager and E. C. Seltzer, Nucl. Data Tables A4, 1 (1968).

[15]E. Newman, K. S. Toth, R. L. Auble, R. M. Gaedke, M. F. Roche, and B. H. Wildenthal, Phys. Rev. C 1, 1118 (1970).

[16]N. de Takacsy and S. Das Gupta, Phys. Rev. C 13, 399 (1976).

[17]C. M. Lederer and V. S. Shirley, *Table of Isotopes*, *7th* ed. (Wiley, New York, 1978).

[18]R. E. Eppley, Wm. C. McHarris, and W. H. Kelly, Phys. Rev. C 3, 282 (1971).

[19]F. Iachello and O. Scholten, Phys. Rev. Lett. 43, 679 (1979).

[20]J. Gizon, A. Gizon, R. M. Diamond, and F. S. Stephens, J. Phys. G 4, 1171 (1978).